AD-A141 261 CORROSION FATIGUE CRACK GROWTH RATES OF WELDMENTS IN Q1N STEEL(U) DDMIRALTY MARINE TECHNOLOGY ESTABLISHMENT POOLE (ENGLAND) B F JONES ET AL. JUN 83 AMTE(M)-R83003 1/1

UNCLASSIFIED DRIC-BR-90072 F/G 11/6 NL

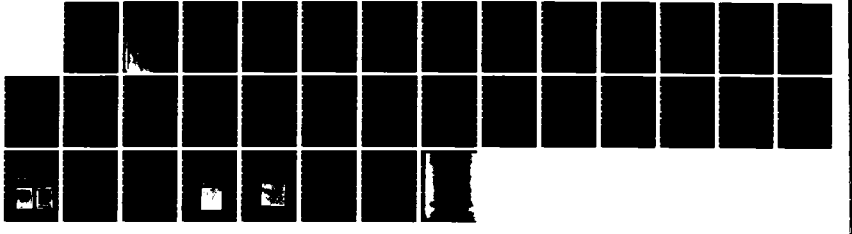

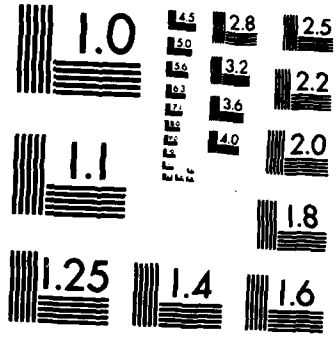

MICROCOPY RESOLUTION TEST CHART
NATIONAL BUREAU OF STANDARDS-1963-A

REPORT AMTE(M)-R 83003

COPY No (2)

AMTE(M) R 83003

ADMIRALTY MARINE TECHNOLOGY ESTABLISHMENT

CORROSION FATIGUE CRACK GROWTH RATES OF WELDMENTS IN QIN STEEL

B F Jones J C Galsworthy

AMTE (Holton Heath)
Holton Heath POOLE
BH16 6JU

JUNE 1983

AMTE(M) R 83003

CORROSION FATIGUE CRACK GROWTH RATES OF WELDMENTS IN Q1N STEEL

by

B F JONES and J C GALSWORTHY

SUMMARY

Low frequency fatigue crack growth rates in air and seawater are reported for manual metal arc, synergic metal inert gas, electron beam and laser beam welds in Q1N steel. The stress corrosion crack growth susceptibility in seawater of the weldments was also studied and both the electron beam and laser beam welds exhibited susceptibility whilst the other welds and parent steel did not. All welds except the 'as-welded' laser beam welds showed similar fatigue crack growth rates to the parent plate. When tested in seawater the laser beam weld was found to exhibit exceptionally fast crack growth rates. The factors influencing fatigue crack growth in weldments are discussed.

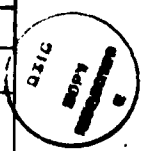

MATERIALS AND LIFE SCIENCES DEPARTMENT
AMTE (HOLTON HEATH)
HOLTON HEATH
POOLE DORSET BH16 6JU

June 1983

INTRODUCTION

1. The majority of fatigue crack growth studies have been conducted on parent metal. Relatively few studies have been conducted on weldments despite the fact that it is probably in association with welds that the sharp defects likely to act as crack initiators will occur. For structures which operate in a marine environment there are the additional problems of corrosion fatigue and stress corrosion crack growth.

2. The problems associated with welding steels to produce joints which match the strength and toughness of the parent metal increase with the yield strength of the steel, especially when for reasons of cost or scale, post weld heat treatment (PWHT) is not applied. Q1N is a medium strength (550 MNm^{-2} yield) low carbon structural steel, generally used in heavy sections (20-40 mm thick) for marine fabrications. It derives its strength and toughness from a specific heat treatment to produce a microstructure of tempered martensite. Although various welding methods and consumables have been developed for this steel, it is hardly surprising that in the as-welded condition, if the strength of the weld is matched to that of the plate, the toughness of the joint is inferior to that of the parent steel. This situation has led to a continuing quest for improved welding methods, procedures and consumables.

3. At present a variety of multipass welding processes such as manual metal arc and submerged arc welding are applied to Q1N. A more recent development has been the application of the synergic metal inert gas technique which promises improved properties. Any multipass welding method has the advantage of providing some degree of tempering to previous weld runs as the weld is built up.

4. High energy, narrow gap, joining processes such as electron beam or laser beam welding offer certain potential benefits compared to more conventional methods. In particular, welding speeds can be extremely rapid, and the total heat input is small thus minimising distortion and with certain susceptible steels freedom from some types of cracking. A further advantage is the elimination of the requirement for a filler material provided a sufficiently narrow weld gap can be achieved. Electron beam welding must be conducted in a vacuum chamber (although out of chamber techniques are being developed) and whilst this is a constraint it has certain advantages in

ensuring clean welding conditions and eliminating gaseous contamination. Deep welds of the order 100-250 mm or greater can be achieved in steel with a single pass by this process. Although laser beam welds can be accomplished without the constraining requirement of high vacuum, single pass penetration is limited to 10-20 mm for a good quality weld in steel at the laser powers readily available at present.

5. The advantages of single pass, autogenous welds are offset for many steels by the absence of tempering which accompanies the multipass processes. The fusion zones of laser or electron beam welds are cooled extremely rapidly by the large surrounding heat sink, leading to a quenched structure of high hardness. Despite this, acceptable levels of toughness have been achieved in as-welded joints encouraging further development of the process.

6. Most published literature(eg 1-5) suggest that the rate of fatigue crack growth in weldments is equal to or less than in the base metal. A few studies have indicated faster crack growth rates for weldments compared to parent plate, but in these instances the differences were only large at near threshold stress intensity ranges(6,7) and high stress ratios(8). A recent survey of ship structural steels(9) concludes 'Overall, the data indicate that corrosion fatigue crack growth rates are no higher in weld metal than in base metal for these steels in marine environments.' However, the evidence on which this general conclusion is based is not always clear as to the nature of the weld studied, or the details of the test conditions (eg specimen type and orientation, test frequency, environment, ΔK range or stress ratio).

7. This report provides the results of comparative tests on a range of welds in Q1N steel. The welds studied were:

a. Manual metal arc (MMA).

b. Synergic metal inert gas (MIG).

c. Electron beam (EB) and

d. Laser beam (LB).

EXPERIMENTAL

Material

8. Parent. The parent material for all welds was Q1N steel which has been well characterised by the test methods described in this report. Although the various types of weld were made using plates from different casts, all complied with the Q1N specification of Table 1. All welds were made with the welding direction parallel to the rolling direction of the parent plate.

9. Manual Metal Arc Weld. Welding details for the MMA weld on a 40 mm thick plate are shown in Table 2. A 'K' preparation was used to provide a straight heat affected zone (HAZ) on one side of the weld (Figure 1a). The conditions used were those which had been shown to provide a weld with slightly overmatching yield strength and a Charpy 'vee' notch impact energy (C_V) which exceeds 60 J at -20°C.

10. Synergic Metal Inert Gas Weld. A 40 mm thick plate was used for the MIG weld and the details are shown in Table 2 and Figure 1b. The conditions used have been found to give good quality welds which slightly overmatch the yield strength of the parent steel and give C_V values of better than 90 J at -20°C.

11. Electron Beam Weld. The welding conditions for the single pass EB weld on 40 mm thick plate are shown in Table 3. These conditions provided a sound weld with a very hard fusion zone which well overmatches the parent steel yield strength and has a C_V of about 45 J at -20°C. However, it should be noted that this welding process has not yet been optimised to the same extent as the MMA and MIG welds with which it is being compared.

12. Laser Beam Weld. Table 4 shows the welding conditions used for the LB weld on 12 mm thick Q1N plate. It is stressed again that the welding conditions may not represent the optimum but do provide sound welds of high hardness and hence overmatching strength with C_V of about 40 J at -20°C.

13. Hardness measurements were made across each of the welds and the profiles are reproduced in Figure 2. The relatively low hardness of the multipass MMA and MIG welds contrasts with the high fusion zone hardness of the single pass EB and LB welds.

14. Some welds were given a PWHT of 1 h at 600°C followed by an air cool. The influence of the heat treatment on the hardness profile was determined and is shown in Figure 2.

Fatigue Testing

15. Single edge-notched cantilever beam specimens (Figure 3) were machined from the welds. Details of the specimen design and stress intensity calibration have been discussed elsewhere[10]. The orientation of the specimens in relation to the welds are illustrated in Figure 4. For the three welds in 40 mm plate (MMA, MIG and EB) specimens were machined as shown in Figure 4a. For the LB weld as much of the weld as possible was used to produce a slightly undersize specimen 10.8 mm wide compared to 12.7 mm for the other welds, machined in the same orientation (Figure 4b). The shallow tapered sidegrooves were omitted from the narrower LB specimens and the stress intensity calibration adjusted accordingly.

16. All specimens were precracked in air at a frequency of 200 cycles per minute (cpm) to a depth of about 1.6 mm using a constant deflection three point bend fatigue machine. During precracking the maximum stress intensity at the precrack tip never exceeded 23 $MNm^{-3/2}$.

17. Low frequency fatigue tests were conducted in the AMTE Flotation Fatigue machines at a frequency of 0.5 cpm (0.008 Hz) using a trapezoidal waveform and R = 0 (where R is the ratio of minimum to maximum load)[10]. These conditions have been shown to produce a significant effect of environment on crack growth rates in the parent material[10,11]. Tests were conducted in laboratory air at ambient temperature and humidity, or in circulating aerated natural seawater obtained weekly from the English Channel. Each batch of seawater was checked on receipt to ensure that the salinity and pH remained within the ranges 3.2 - 3.5% and 7.7 - 8.1 respectively.

18. Crack depths were monitored using a calibrated direct current electrical resistance technique (DCPD) which gave an estimated resolution of ±0.05 mm. Separate calibrations were made for each of the welds studied. All other experimental details have been described elsewhere[10], and it is noted that the crack growth rates presented are for 'steady state' conditions as apparent 'incubation' and transient effects have been eliminated by appropriate selection of the data[10,11].

Stress Corrosion Testing

19. Limited stress corrosion testing was undertaken using identical precracked specimens to those used for corrosion fatigue tests, and the environment of circulating aerated natural seawater. Specimens were subjected to a constant load which provided a stress intensity of 50 $MNm^{-3/2}$ at the precrack tip and crack depth was monitored by DCPD.

RESULTS

20. The fatigue crack growth rates for the four welds are shown in Figures 5-8. The curves drawn on these plots represent the scatter band determined for parent Q1N from a large number of tests[10].

21. Figure 5a shows that the as-welded MMA specimens exhibited air crack growth rates at the low end of or lower than the parent plate scatter band. A similar enhancement occurs for the weld as for the parent plate when the tests are conducted in seawater - the as-welded specimen growth rates still being less than for parent material (Figure 5b). The influence of the PWHT is to eliminate the differences in growth rate between parent plate and weldment, resulting in an increase in the weld metal growth rate to within the parent plate scatter band for both air and seawater respectively.

22. The as-welded properties of the MIG welds are very similar to those of the parent plate (Figure 6) and a little faster than those recorded in Figure 5 for the MMA weld, the enhancement due to seawater remaining the same. PWHT produced a less distinct increase in crack growth rate for the MIG weld, but still large enough to provide some values slightly above the parent plate scatter band, especially in air at lower ΔK.

23. The results for EB welds are shown in Figure 7. No PWHT was performed on this material. Air crack growth rates slightly exceed the parent plate scatter band at lower ΔK (<30 $MNm^{-3/2}$) but fall at the lower extreme at higher ΔK (>40 $MNm^{-3/2}$) - Figure 7a. The seawater crack growth rates of Figure 7b show greater scatter in growth rates compared to the parent plate over the whole ΔK range studied.

24. Figure 8 shows the fatigue crack growth rates for the LB weld. Only one test was conducted in air and Figure 8a indicates growth rates within the parent plate scatter band except at the lowest ΔK value. The seawater data of Figure 8b show the greatest scatter of any of the welds studied with some

specimens showing rates as much as 4x faster than the parent plate and another showing rates well below the minimum of the parent plate scatter band. However, those specimens which had been given a PWHT exhibited growth rates within the scatter band for parent plate.

25. Stress corrosion tests loaded to a stress intensity of 50 $MNm^{-3/2}$ at the tip of the precrack have shown no evidence of crack extension for parent plate, MMA weld and MIG weld after exposure for 6000 h, 3500 h and 9200 h respectively. Based on the estimated capability of the DCPD system to detect crack extension of the order of 0.05 mm, the stress corrosion crack growth rates for these materials is less than 2.5×10^{-9}, 4.0×10^{-9} and 2.7×10^{-9} mm s^{-1} respectively.

26. An EB weld tested under identical conditions failed in 2266 h. A second EB specimen was loaded at an initial stress intensity of 45 $MNm^{-3/2}$ and this failed in 3174 h.

27. An LB weld loaded to an initial stress intensity of 50 $MNm^{-3/2}$ failed in 6056 h.

28. Both EB and LB weld specimens exhibited typical stress corrosion crack growth rate 'plateaux' which were about 10^{-6} mm s^{-1} at 55 $MNm^{-3/2}$.

DISCUSSION

29. The air fatigue crack growth rates for all welds are similar to those of parent Q1N. There is evidence that at low ΔK the rates are slightly faster for the EB and LB welds compared to parent Q1N and it is certainly the case that these welds exhibit faster air crack growth rates than the MMA or MIG welds. Two possible explanations for this are discussed below.

30. It may be that the composition, microstructure and strength level of the EB and LB welds makes them more sensitive to water vapour in the ambient environment than the other materials involved. Such sensitivity has been demonstrated for a similar material[12] and the high hardness of the fusion zone of the EB and LB welds (Figure 2) might result in a degree of sensitivity to moisture, as is suggested by their susceptibility to stress corrosion crack growth (paragraphs 25-28).

31. Alternatively it might be that the residual or internal stresses present in specimens machined from the different types of weld produce the difference. This explanation relies on the concept of crack closure. As a

fatigue crack under a tensile opening load is unloaded the faces of the crack approach one another and in an ideal solid with no internal stresses and a smooth crack the faces of the crack would meet when the applied load is zero - the application of a compressive load across the crack would not cause additional movement of the crack faces and thus not contribute to the fatigue cycle. In practice there are several factors which change this situation[12,13]. The degree of opening at any applied load can be influenced by plasticity induced internal stress related to plastic deformation at the crack tip and the work hardened or softened material left in the wake of the crack. These effects are especially significant under plane stress loading conditions when plastic zones are larger. More recently the idea of roughness and oxide induced closure has been introduced, whereby the rough oxide coated surfaces of a fatigue crack might tend to interfere before the cyclic load reaches zero, thus reducing the effective load range[13]. A similar reduction in effective load range could also be produced if an internal compressive stress were present in the specimen and was superimposed in the applied stress cycle. These residual or internal stresses are likely to differ in specimens cut from the different types of weld and this might explain the present results if the specimens from the MMA and MIG welds contained larger compressive stresses at the crack tip than the EB and LB welds. In this respect it is noteworthy that the MMA weld which exhibits the slowest of the as-welded fatigue crack growth rates also exhibits clear evidence of crack edge lagging (Figure 9a) whereas the MIG, EB and LB welds all showed relatively straight crack fronts (Figures 9b, c and d), although the EB and LB welds obviously grew faster at one edge of the specimen compared to the other.

32. PWHT resulted in an increase in the air fatigue crack growth rate for both MMA and MIG welds. In the case of the MMA weld this was accompanied by a straightening of the crack front which might be attributed to a reduction in residual stress. Comparison of the microstructure and hardness of the fusion zone before and after PWHT suggests that the microstructure is not greatly altered. In the case of the MIG weld the fatigue crack growth rates after PWHT are slightly above the upper bound of the parent plate scatter band. The reason for this is not yet understood, and has prompted additional studies of the MIG weld. Unfortunately, there was insufficient EB and LB material to permit studies of the air fatigue crack growth rates after PWHT.

33. All welds exhibited an increase in fatigue crack growth rate when tested in seawater, and in the case of MMA, MIG and EB welds the rates were similar to those measured for Q1N. The slight differences in the seawater rates for the parent Q1N, MMA and MIG welds were in the same sense as was observed in the air tests, and PWHT had a similar effect (see Figures 5 and 6).

34. It is interesting to note that when tests are conducted in seawater at R = 0.5 the results for the parent plate, as-welded MMA and MIG welds and PWHT MMA and MIG welds fall within a much tighter scatter band than could be drawn for R = 0 tests (Figure 10). Growth rates for all materials are faster at R = 0.5 compared to R = 0, but those for the as-welded MMA weld increase by a greater amount than the parent plate or other welded materials. This provides strong evidence that closure effects caused by residual compressive stresses and corrosion product/surface roughness interference are the main reason for the differences in growth rate observed in the R = 0 tests - the higher stress ratio (ie $K_{min} > 0$) eliminating closure at the minimum of the load cycle. Further supporting evidence of crack closure in R = 0 tests comes from comparison of DCPD readings taken at the maximum and minimum of the load cycle. In air tests a continuous insulating air oxide film on the surfaces of the crack means that identical PD readings are obtained whether the crack is fully opened (maximum load) or closed (minimum load). When tests are conducted in seawater the air oxide film dissolves in the first few days[14] and is replaced by other corrosion products. The result is that the off load PD decreases due to conductivity between the crack faces, implying intimate contact of the faces. However, in the tests conducted in seawater at R = 0.5, the DCPD readings at maximum and minimum load remain the same, suggesting that the crack faces no longer come into contact and conduct at minimum load.

35. The seawater crack growth rates for the EB weld show greater scatter than those of the multipass welds with some values slightly above and others slightly below the parent plate scatter band. The as LB welded specimens are the only ones which show some crack growth rates significantly faster than for parent plate. PWHT resulted in crack growth rates within the parent plate scatter band and a reduction in the hardness of the fusion zone, although it remained considerably harder than the parent plate (Figure 2).

36. The rapid and widely scatte corrosion fatigue crack growth rates for the as LB welded specimens prom ed a detailed analysis of the fatigue frac-

tures in relation to the structure of the weld. Macroscopically the LB weld was observed to exhibit a distinct centreline, presumably representing the junction of elongated columnar grains growing from the weld edges (Figure 11). Examination of individual specimens revealed that the growth rates measured in seawater were critically dependent upon the position of the original edge notch in relation to the weld centreline. When the root of the notch was sufficiently close to the weld centreline for the fatigue crack to grow in this feature (as in Figure 12a), then extremely fast seawater fatigue crack growth rates were measured and flat fatigue fracture surfaces observed (Figure 12b). However, when the notch was remote from the weld centreline, and crack growth did not coincide with the centreline (Figure 13a), much slower fatigue crack growth rates were recorded in seawater, and the fracture surface was rougher and revealed much crack branching and secondary cracking (Figure 13b).

37. The air fatigue test conducted on an as LB welded specimen cracked down the weld centreline but did not exhibit exceptional crack growth rates. Similarly, of two LB welded specimens tested in seawater after PWHT one cracked in the weld centreline and the second close to it, but both exhibited crack growth rates within the 'normal' scatter band.

38. In view of these observations it appears likely that the rapid crack growth rates observed for LB welds in seawater are as a consequence of the extreme environmental sensitivity of columnar (or interdendritic) grain boundaries. In the centreline of the weld these boundaries are aligned parallel with the crack growth direction and provide an effective path for rapid crack growth. However, when the crack is remote from the centreline it encounters the columnar boundaries at right angles to the crack growth direction - crack branching results, causing an effective reduction in crack tip stress intensity and growth rate. Figure 13b provides a good illustration of this point as the features outlined by the secondary cracks are of the same order as the columnar grain diameter.

39. Previous evidence that columnar (or dendrite) boundaries might be sensitive to environmental cracking has been provided by Vosikovsky[8] who studied a deep weld accomplished in two passes in a 12.7 mm thick HY130 plate by the automatic gas metal arc (MIG) process. He noted a tendency for rapid 'interdendritic cracking' in fatigue crack growth tests conducted in 3.5% sodium chloride solution.

40. The occurrence of enhanced corrosion fatigue crack growth rates in the high hardness fusion zone of LB welds and the relatively low ΔK sensitivity of growth rate above the knee of the fatigue crack growth rate curves encourages the view that this material is showing characteristics typical of corrosion fatigue crack growth 'above K_{ISCC}'(eg 15). However, although stress corrosion cracking was observed in the LB weld it was very slow at $K = 50\ MNm^{-3/2}$, suggesting that the threshold (K_{ISCC}) would not be much less than this value. Despite this, rapid corrosion fatigue crack growth rates (between 5-10x faster on a time rather than cyclic base) were recorded for $\Delta K = K_{max}$ as low as $25\ MNm^{-3/2}$. Furthermore, the flat centreline cracking typical of the rapid fatigue crack growth rates was not reflected in the stress corrosion failure which showed an extremely irregular crack path despite the crack starting close to the centreline and intersecting the centreline at several points as it grew.

41. The simple interpretation of a direct correlation between stress corrosion crack growth susceptibility and rapid corrosion fatigue crack growth is further confounded by the observation that whilst exhibiting a sensitivity to stress corrosion the as EB welded material did not show any large enhancement of corrosion fatigue crack growth rate even at $\Delta K > 50\ MNm^{-3/2}$ with cracking in the weld centreline.

42. The fact that the as-welded specimens prepared by both the EB and LB processes exhibited identical high hardness suggests that there is no direct correlation of hardness with the rapid corrosion fatigue crack growth rates. Although the structures of the EB and LB welds are similar, it is noted that the appearance of their centrelines was different (Figures 11b and 14). Thus the explanation of the difference between the corrosion fatigue crack growth rates for the two single pass welds may be that the LB weld provides relatively continuous, parallel environmentally sensitive interdendritic boundaries in the centreline, whereas these boundaries may be less continuous (and possibly less sensitive to the environment) in the instance of the EB weld. A less consistent centreline may explain why the EB weld showed considerable scatter in crack growth rates. In the instance of the LB weld, the importance of the fatigue cycle in producing exceptional crack growth rates (compared to stress corrosion crack growth) may be that it provides a mechanism for linking closely adjacent (but not continuous) and suitably oriented interdendritic boundaries.

43. The reason for the environmental sensitivity of the interdendritic boundaries has not been identified. Scans across both LB and EB welds with an electron probe microanalyser have failed to identify any significant compositional variation associated with the centreline of the welds. However, if there is segregation of species to interdendritic boundaries, then the significance of the centreline would be in the alignment of the boundaries parallel to the crack growth direction, and an equivalent degree of segregation might be anticipated at such boundaries away from the centreline.

44. The fact that PWHT at 600°C reduces the environmental sensitivity of the boundaries suggests that the characteristics of the problem may be similar to the embrittlement of grain boundaries arising from the segregation of impurity elements such as P, S, Sb, Sn, etc either during austenitising or subsequent tempering treatments (temper-embrittlement). It is well known that P can segregate at austenitising temperatures[16], and a correlation between the segregation of such elements and stress corrosion crack growth[17,18] and corrosion fatigue crack growth[11] has been identified. A heat treatment at 600°C is normally observed to reduce the embrittlement, presumably by redistribution of the previously segregated elements.

45. It may well be that the segregation of embrittling species is encouraged by the presence of other elements or compounds at dendrite boundaries. This could arise if, as a result of extremely rapid heating and cooling associated with laser welding in particular, certain high melting point non-metallic constituents were never completely dissolved and hence segregated during solidification of the fusion zone.

46. It is noted that poor impact toughness has sometimes been associated with centreline cracking in EB and LB welds in steels of this type[17]. In such cases the fracture surfaces exhibit interdendritic separation and the cause may, therefore, be closely related to the environmental sensitive corrosion fatigue cracking observed in the LB weld. It seems most likely that Auger spectroscopic examination of fast fracture surfaces may reveal the nature of the segregated species.

47. The application of fracture mechanics assessment methods to structural fabrications usually requires a knowledge of the fatigue crack growth properties of the materials of construction. The results presented in this paper illustrate the problems associated with the measurement of fatigue and corro-

sion fatigue crack growth rates of welds. This is especially serious where the size of the structure means that tests cannot be undertaken on the complete component.

48. Where residual welding stresses are concerned it is clearly unlikely that the real weld and a test specimen will contain the same pattern or magnitude of internal stresses. Even when the scale and geometry of the real joint is reproduced in the test weld, the machining of a test specimen will cause modification of the internal stresses. Thus, the aim must be to measure the properties of the materials of a weldment independently of internal stresses, and to measure separately or estimate the stress state of the real weld and incorporate this factor by appropriate modification of the applied loads in the fracture mechanics assessment.

49. It is difficult to measure the fatigue properties of any as-fabricated weldment in isolation from the influence of residual stress. Such stresses can be reduced by stress relief heat treatments, but for steels there is the possibility that such treatments will modify the microstructure of the weldment, so that the material being tested is not truly representative of the as-welded material. The results of Figure 10 suggest that testing at higher stress ratios might represent one means of overcoming the effect of residual stresses which influence crack growth by causing crack closure. Such an approach must be treated with caution, however, as high R implies high values of K_{max} where static fracture modes might enhance crack growth rates which would not then be typical of fatigue at low R.

50. Apart from problems of residual stress no weld can be considered completely homogeneous and some consideration must be given to the position and orientation of the crack being measured and to differences in the degree of parent metal dilution effects, tempering and microstructural variations. Such differences seem especially significant in the case of the LB weld where the position of the crack in relation to the weld centreline appears to be critical with respect to crack growth rates in seawater.

CONCLUSIONS

51. Low frequency fatigue crack growth rates in air and seawater have been determined for manual metal arc (MMA), synergic metal inert gas (MIG), electron beam (EB) and laser beam (LB) welds in Q1N steel. The growth rates for the MMA, MIG and EB welds were not greatly different to those of the parent steel.

52. The LB welded steel exhibited extremely rapid crack growth rates in seawater, when the fatigue crack was growing along the centreline of the weld. The exceptional growth rates appear to be related to the extreme environmental sensitivity of interdendritic or intercolumnar grain boundaries.

53. Stress corrosion crack growth was observed for both EB and LB welds but was not found in MMA or MIG welds or in parent plate.

54. Internal stresses in specimens from welds appear to influence crack growth rate, possibly by inducing closure of the crack faces during the positive part of the fatigue cycle during unloading and thus reducing the effective load range below the applied load range.

55. When compared in seawater at R = 0.5, the fatigue crack growth rates for parent plate, MMA and MIG welds (as-welded and after PWHT) show very little scatter, suggesting that such test conditions eliminate the influence of crack closure induced by surface roughness and/or internal stress.

ACKNOWLEDGEMENTS

56. The MMA and MIG welds were provided by AMTE(S) and the EB and LB welds were supplied in the early 1970's by The Welding Institute. The assistance and advice of colleagues in the Ferrous and Non-Ferrous Metallurgy and Electron Optics Sections of the MC Division are gratefully acknowledged, and special mention is made of the contribution of Mr B O'Connor, a vacation student from University College Cardiff, for his work on the laser and electron beam welds.

REFERENCES

1. MADDOX S J. Welding Journal 49 (1970) Research Supplement 445s.
2. CLARK W G Jr and KIM D S. Eng Fracture Mech 4 (1972) 499.
3. SEELEY R R, KATZ L and SMITH R M. ASTM STP 648 (1978) 261.
4. BUCCI R J, GREEN B N and PARIS P C. ASTM STP 536 (1973) 206.
5. ROLFE S T and BARSOM J M. 'Fracture and Fatigue Control in Structures. Applications of Fracture Mechanics' (Prentice Hall Inc, Englewood Cliffs, NJ, 1977) p 252.
6. OHTA A, SASAKI E, KAMAKURA M, NIHEI M, KOSUGE M, KANAO M and INAGAKI M. Trans Japan Welding Soc 12 (1981) 31.
7. OHTA A, SASAKI E, NINEI M, KOSUGE M, KANAO M and INAGAKI M. In J Fatigue, October 1982.
8. VOSIKOVSKY O. Welding Journal 60 (1980) Research Supplement 255s.
9. JASKE C E, PAYER J H and BALINT V S. Corrosion Fatigue of Metals in Marine Environments (Battelle Memorial Institute, Battelle Press, Columbus, Ohio, 1981) p 74.
10. JONES B F. J Mater Sci 17 (1982) 499.
11. JONES B F. Int J of Fatigue, October (1981) 167.
12. JONES B F. AMTE(M) R 82008, December 1982.
13. SURESH S and RITCHIE R O. Metallurgical Transactions 13A (1982) 1627.
14. TOWNSEND H E, CLEARY H J and ALLEGRA L. Corrosion-Nace 37 (1981) 384.
15. AUSTEN I M and WALKER E F. The Influence of Environment on Fatigue. I Mech E Conference Publications 1977-4 (Chameleon Press Ltd, London) 1977, p 1.
16. YU J and McMAHON C J Jr. Metallurgical Transactions 11A (1980) 291.
17. RELLICK J R and McMAHON C J Jr. Metallurgical Transactions 5 (1974) 2439.
18. HONDROS E D and LEA C. Nature 289 (1981) 663.
19. AMTE and The Welding Institute, Unpublished Data.

TABLE 1

SPECIFIED COMPOSITION FOR Q1N PLATE

Element	C	S	P	Si	Mn	Ni	Cr	Mo
Wt %	0.18 max	0.015 max	0.015 max	0.35 max	0.40 max	2.25-3.25	1.0-1.8	0.2-0.6

TABLE 2

WELDING DETAILS FOR MMA AND MIG WELDS

Electrode	Heat Input KJ/mm	Current amps	Voltage volts	Speed mm/min	Run/Electrode (length cm)	No. of Runs	
4 mm Fortrex 11018	1.9	185	20	-	7 of 46	20	MMA
1.2 mm AX90	2.1	155	20.5	77	-	17	MIG

Composition of Electrodes:

Wt %	C	S	P	Si	Mn	Ni	Cr	Mo	Cu	V	Al	Ti	Co
11018 (Range)	0.05-0.07	0.006-0.015	0.008-0.018	0.3-0.5	1.40-1.80	1.47-1.75	0.05-0.35	0.35-0.65	0.02-0.10	0.02-0.16	<0.05	-	-
AX90 (Typical)	0.08	0.012	0.010	0.37	1.42	2.10	0.08	0.44	0.05	0.01	0.012	0.02	0.06

TABLE 3

WELDING DETAILS FOR ELECTRON BEAM WELD

(Single Pass 40 mm Plate)

Accelerating Voltage	150 kV
Beam Current	120 mA
Through Current	30 mA
Travel Speed	150 mm/min
Focus Position wrt Surface	10 mm below
Weld Width (mid point)	5 mm

TABLE 4

WELDING DETAILS FOR LASER BEAM WELD

(Single Pass 12 mm Plate)

Beam Power	11 kW
Travel Speed	750 mm/min
Gas Shield	He
Focus Position wrt Surface	2 mm below

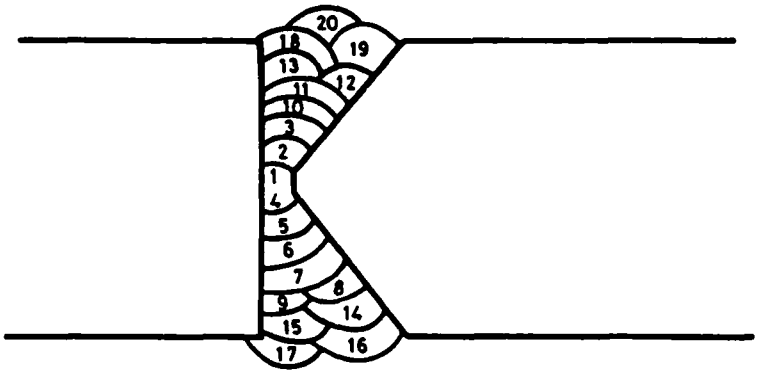

a) MMA Weld

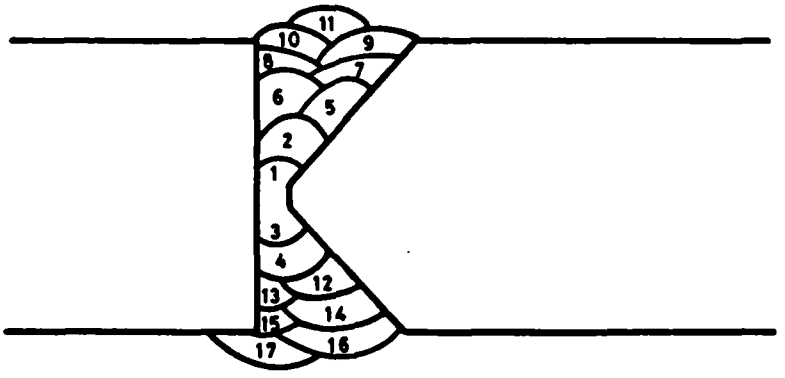

b) MIG Weld

FIG.1. MMA AND MIG WELDS (Schematic).

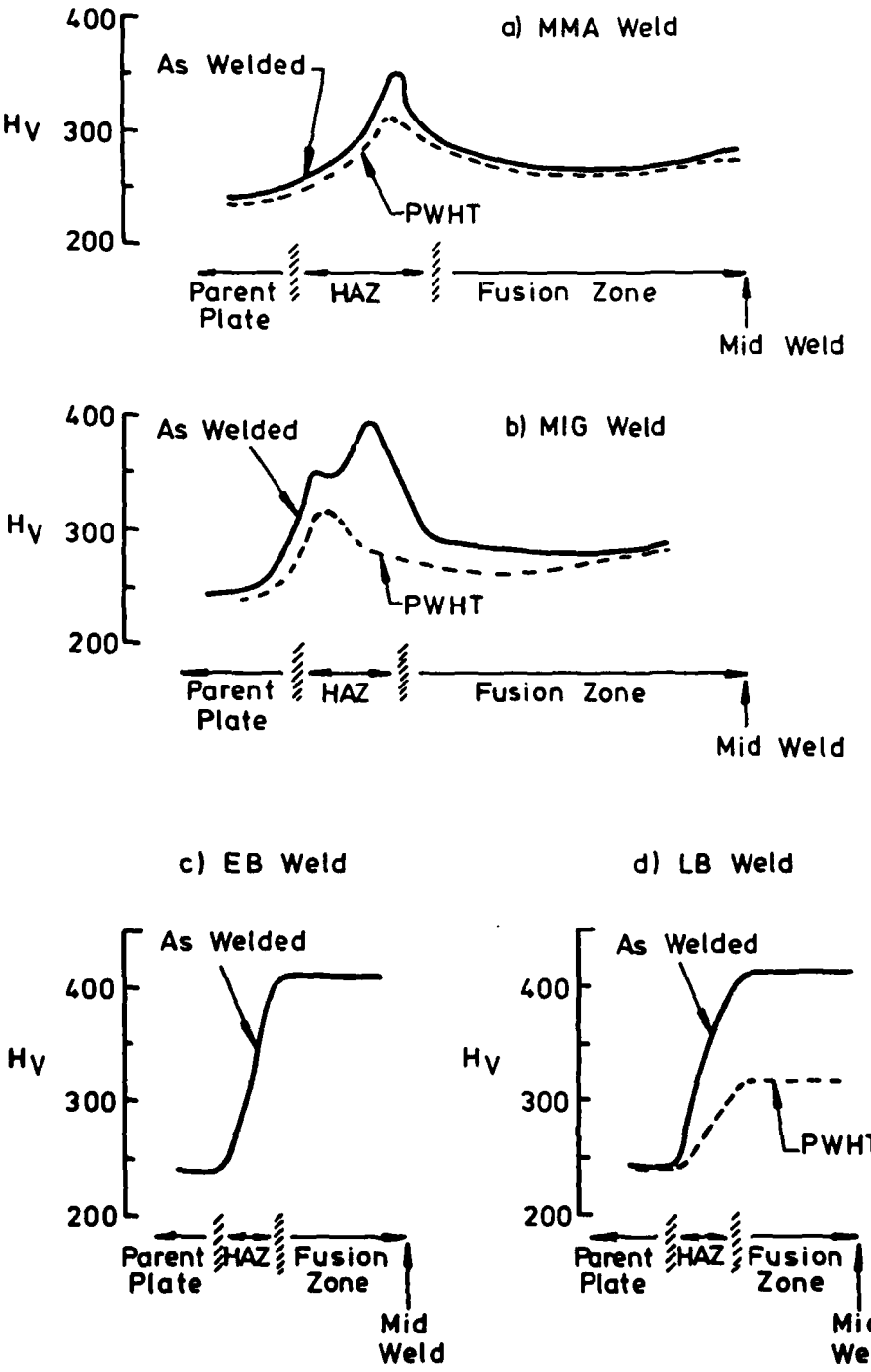

FIG. 2. HARDNESS PROFILES ACROSS WELDS.

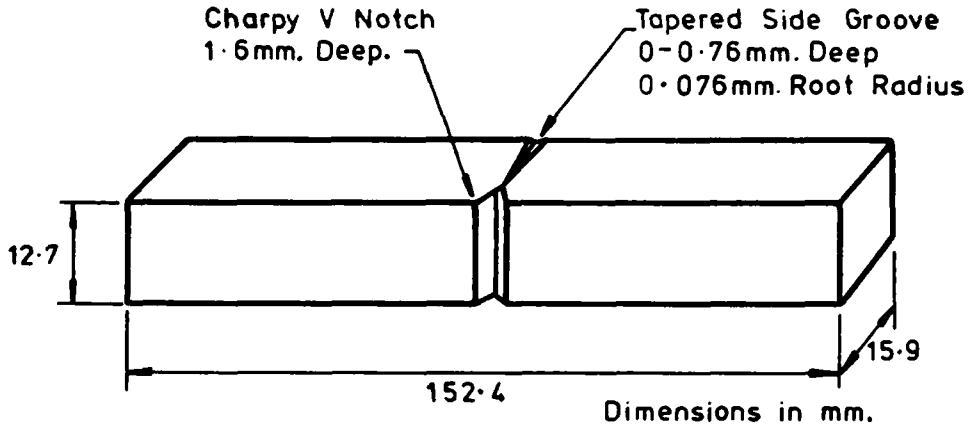

FIG. 3. SEN CANTILEVER BEAM SPECIMEN

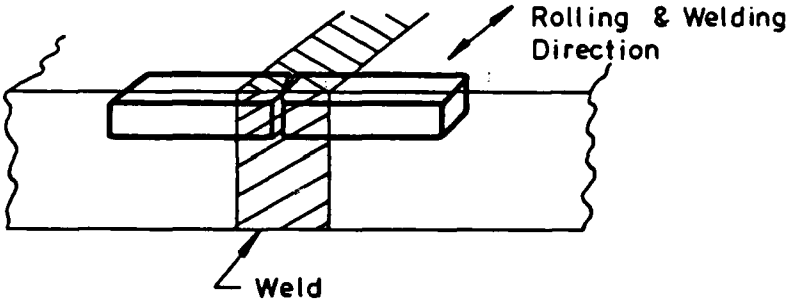

a) MMA, MIG and EB Weld Specimens

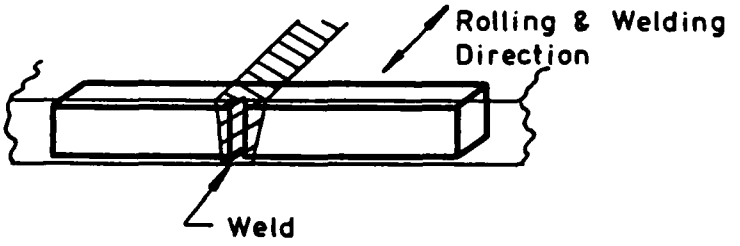

b) LB Weld Specimen (No Side Groove)

FIG. 4. POSITION AND ORIENTATION OF SPECIMENS FROM WELDS.

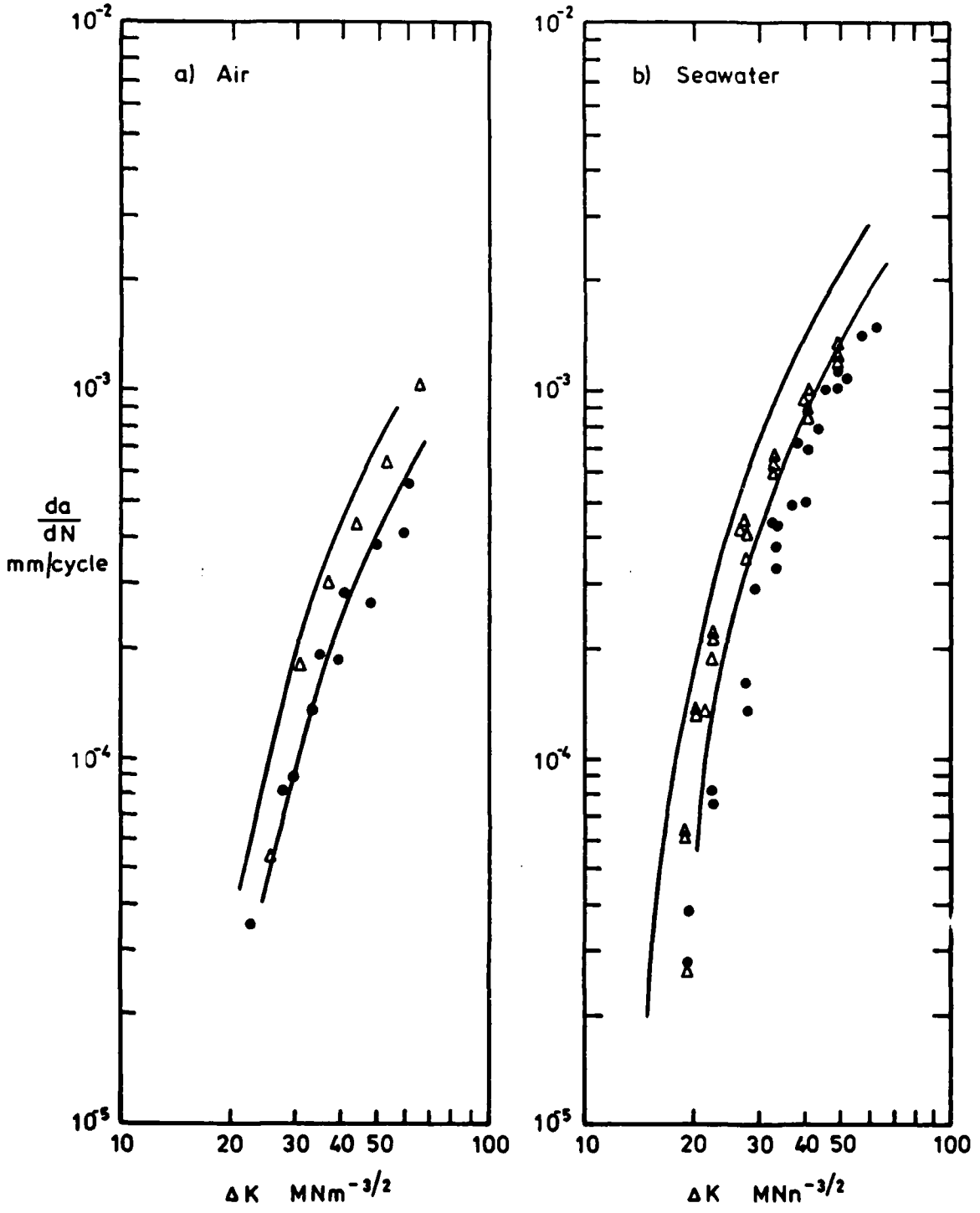

FIG. 5. FATIGUE CRACK GROWTH RATES OF MMA WELD IN a) AIR AND b) SEAWATER. (Frequency 0·5 cpm, R=0, Trapezoidal Waveform).

• As Welded, Δ PWHT, // Parent Plate Scatter Band.

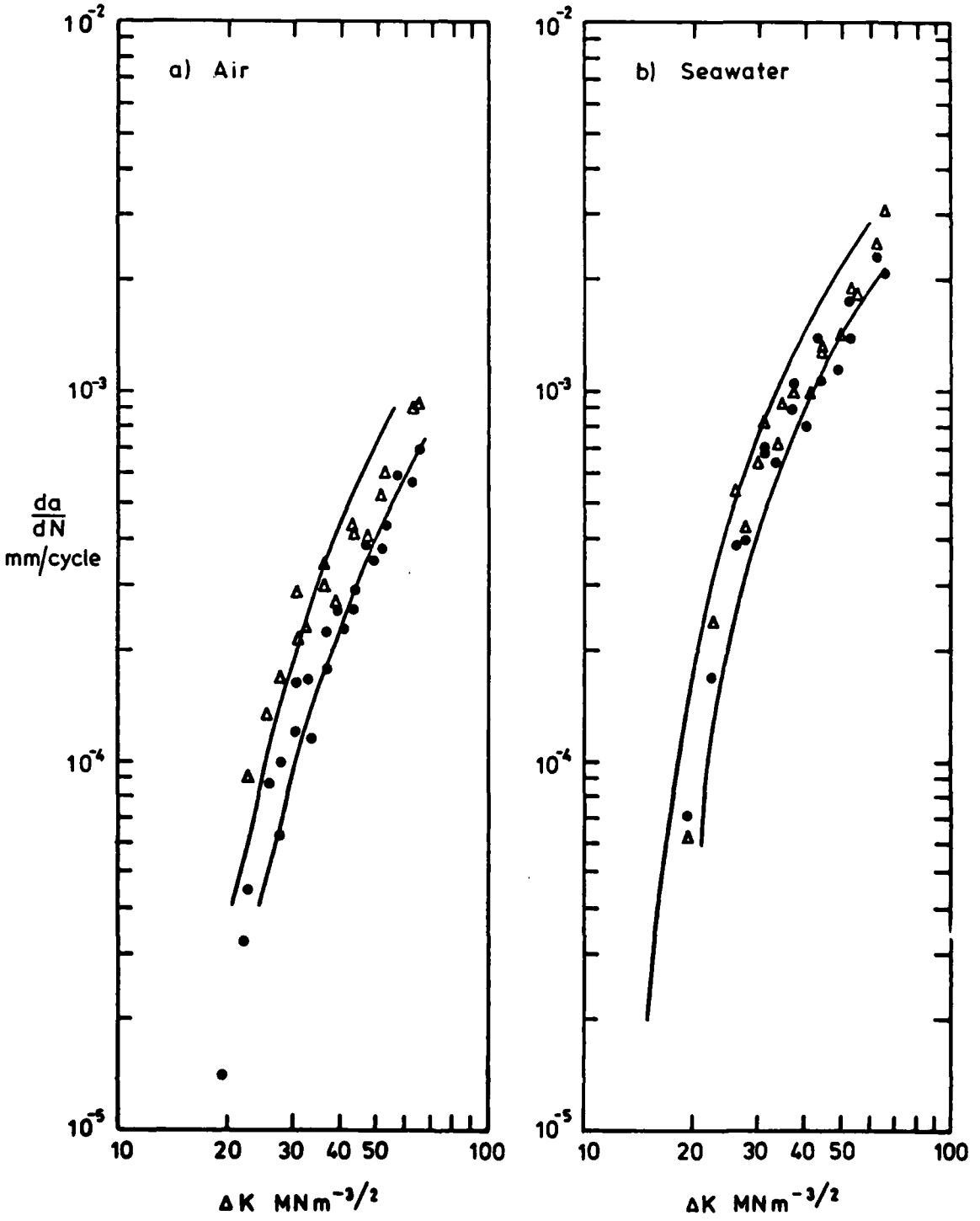

FIG. 6. FATIGUE CRACK GROWTH RATES OF MIG. WELD IN a) AIR AND b) SEAWATER. (Frequency 0·5 cpm, R=0, Trapezoidal Waveform).

• As Welded, Δ PWHT, // Parent Plate Scatter Band.

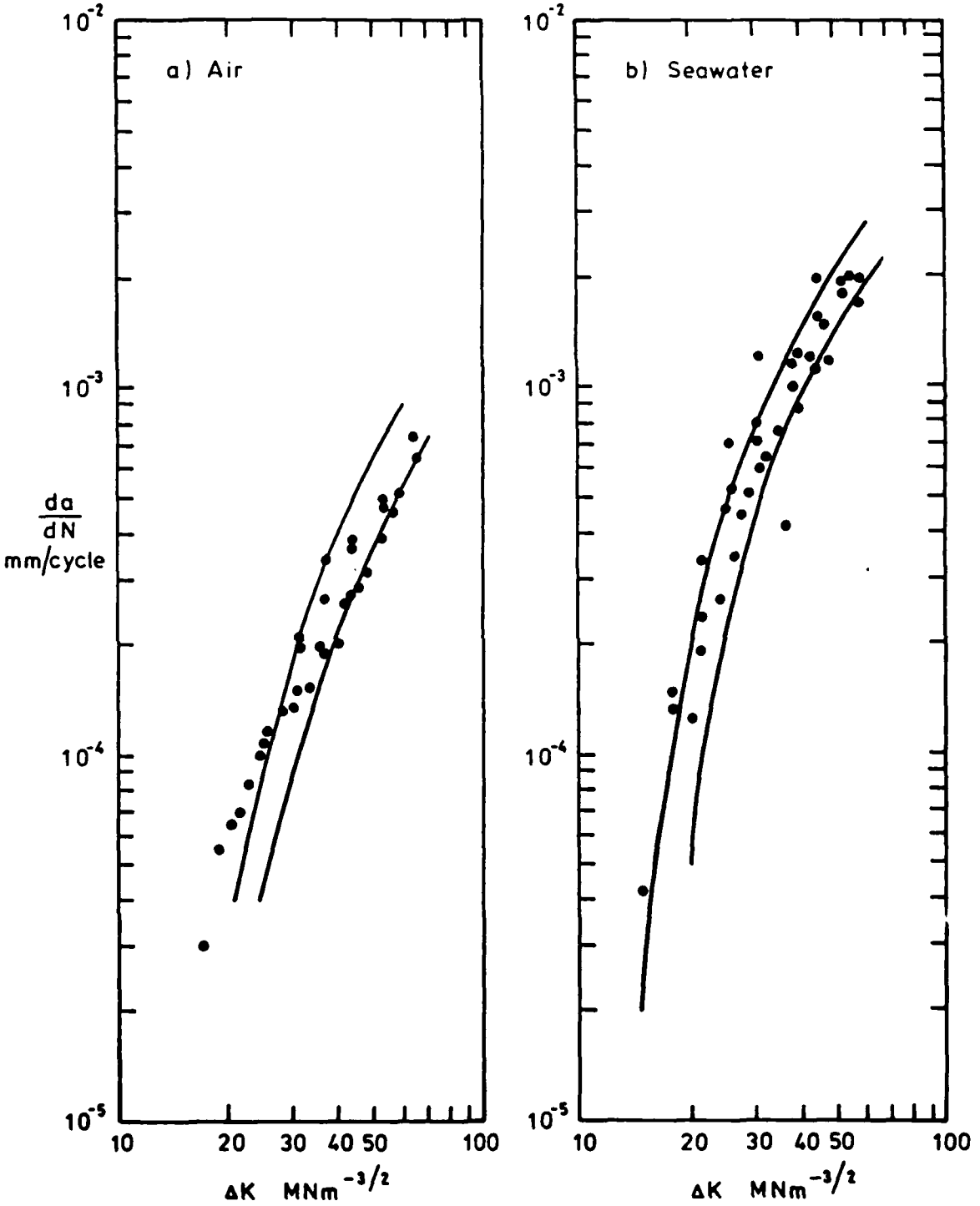

FIG. 7. FATIGUE CRACK GROWTH RATES OF EB WELD IN a) AIR AND b) SEAWATER. (Frequency 0·5 cpm, R = 0, Trapezoidal Waveform).

• As Welded. // Parent Plate Scatter Band.

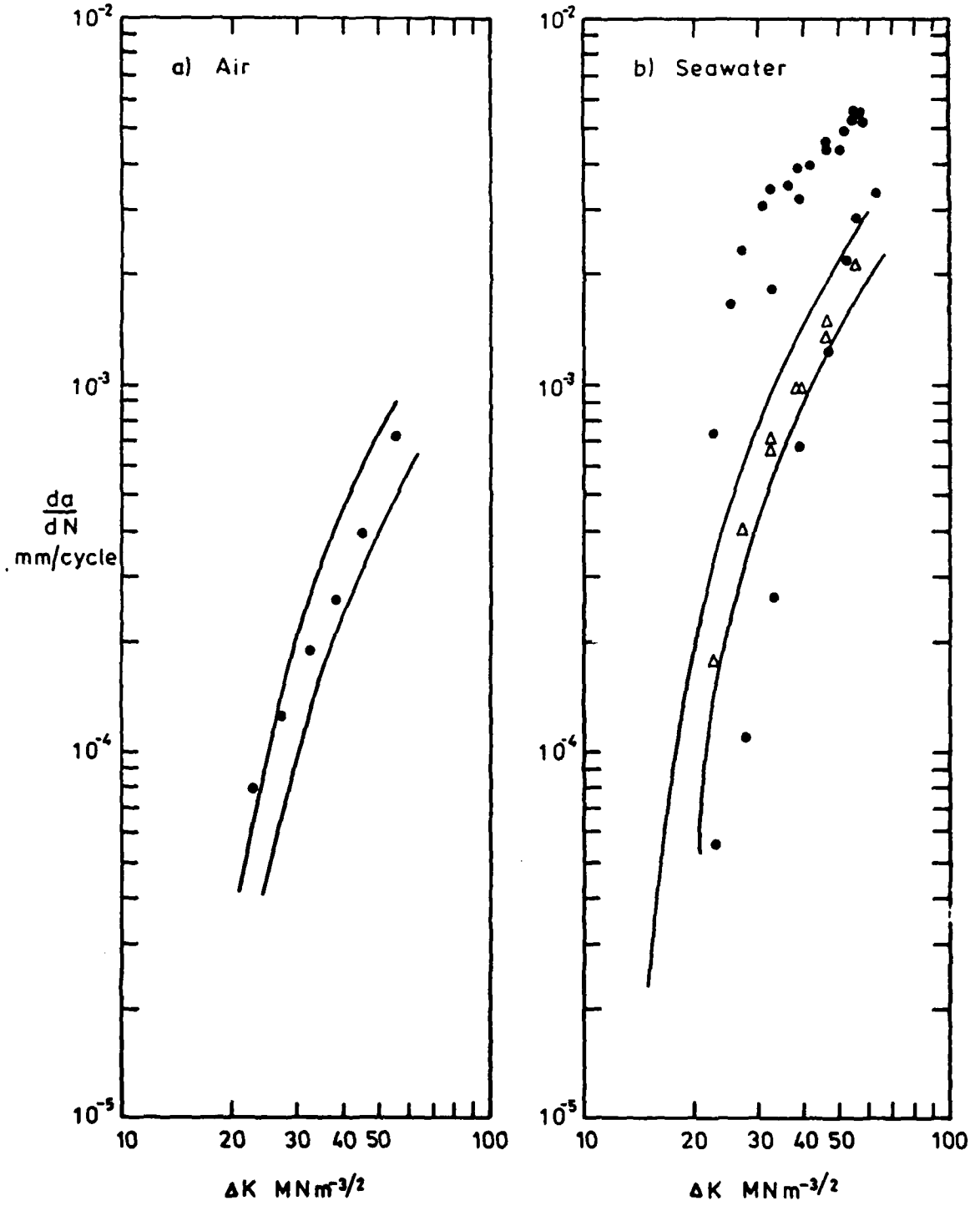

FIG.8. FATIGUE CRACK GROWTH RATES OF LB WELDS IN a) AIR AND b) SEAWATER. (Frequency 0·5 cpm, R=0, Trapezoidal Waveform).

• As Welded, Δ PWHT, // Parent Plate Scatter Band.

a) MMA Weld

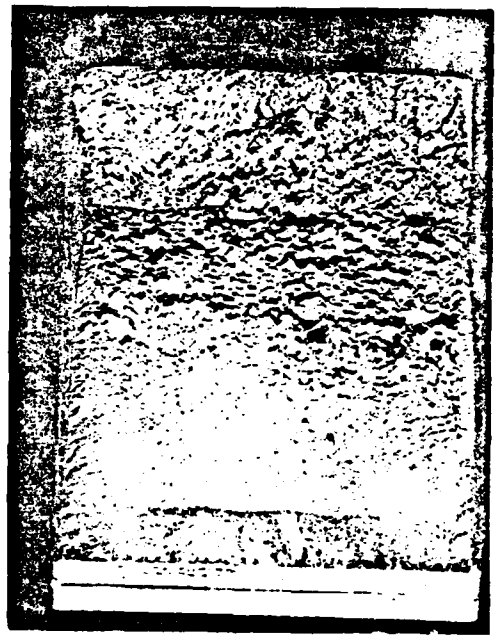

b) MIG Weld

c) EB Weld

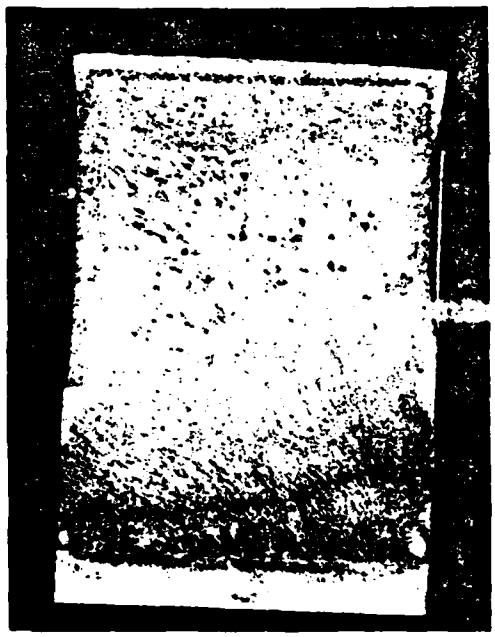

d) LB Weld

FIG 9. CRACK FRONT SHAPES IN WELDS

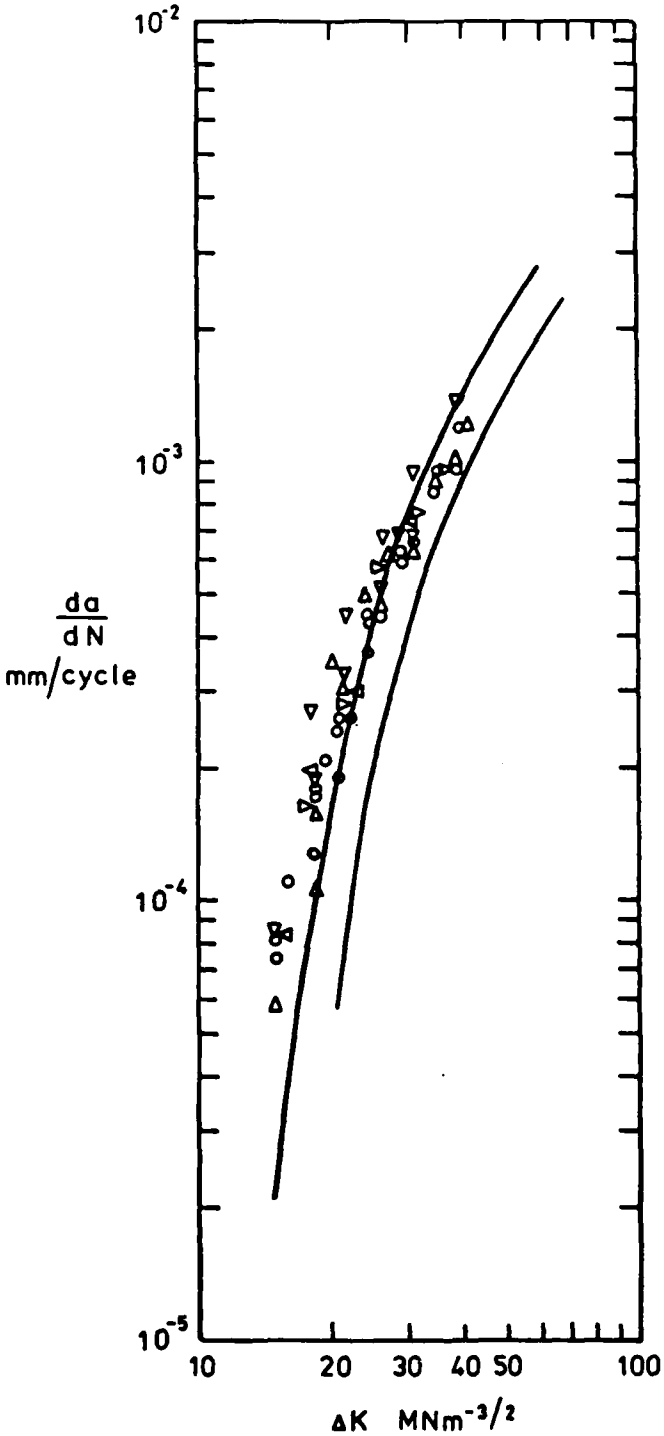

FIG. 10. FATIGUE CRACK GROWTH RATES IN SEAWATER AT R = 0·5 FOR PARENT QIN STEEL AND AS-WELDED AND PWHT, MMA, AND MIG WELDS. (Frequency 0·5 cpm, Trapezoidal Waveform).

- o QIN Parent Plate.
- ▷ As MIG Welded.
- ◁ PWHT MIG Weld. R = 0
- △ As MMA Welded.
- ▽ PWHT MMA Weld.
- // Parent Plate Scatter Band.

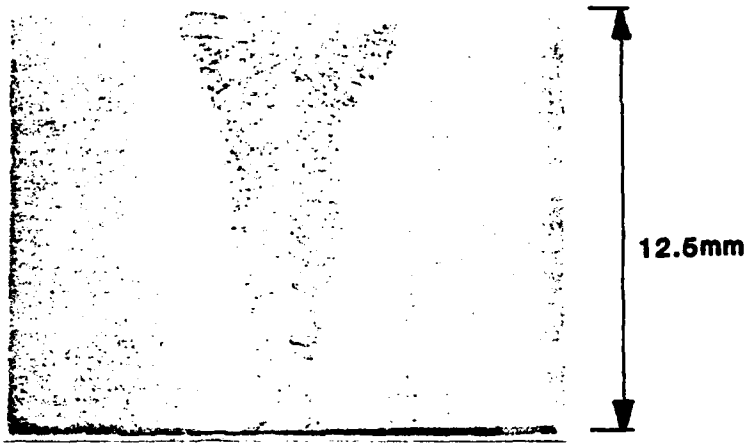

a) Transverse

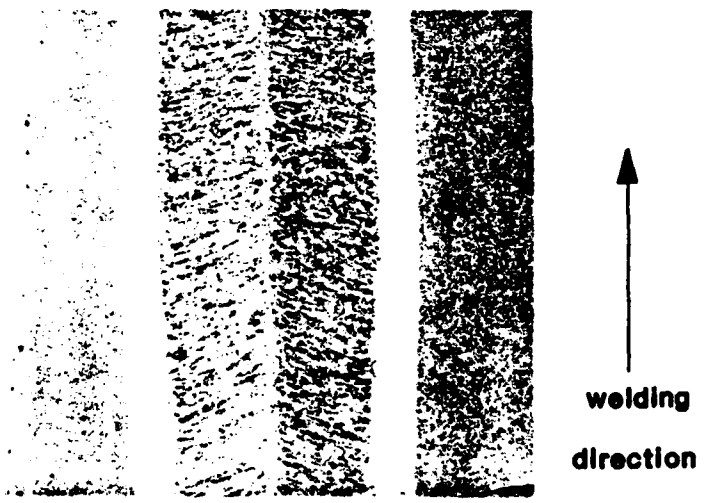

b) Longitudinal

FIG 11. MACRO STRUCTURE OF LB WELD

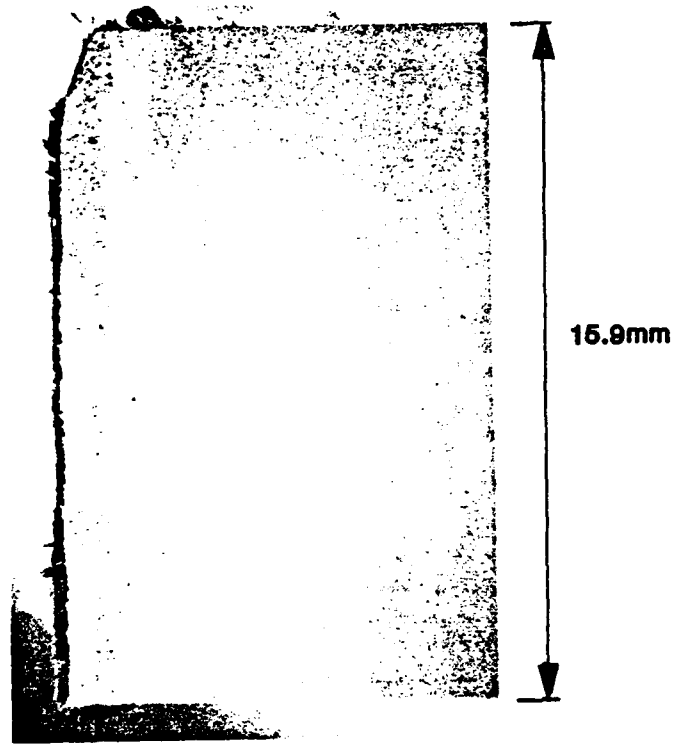

a) Macrograph showing central postion of crack

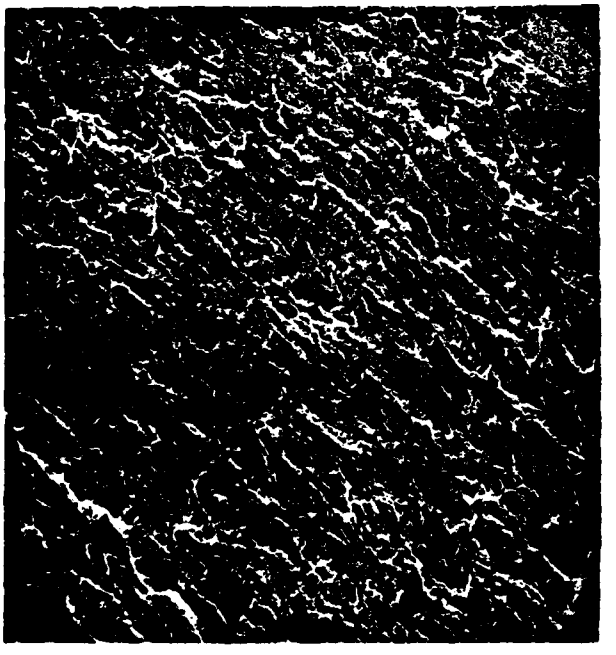

b) Scanning electron micrograph showing smooth fracture surface

FIG 12. CENTRELINE CRACK GROWTH IN LB WELD

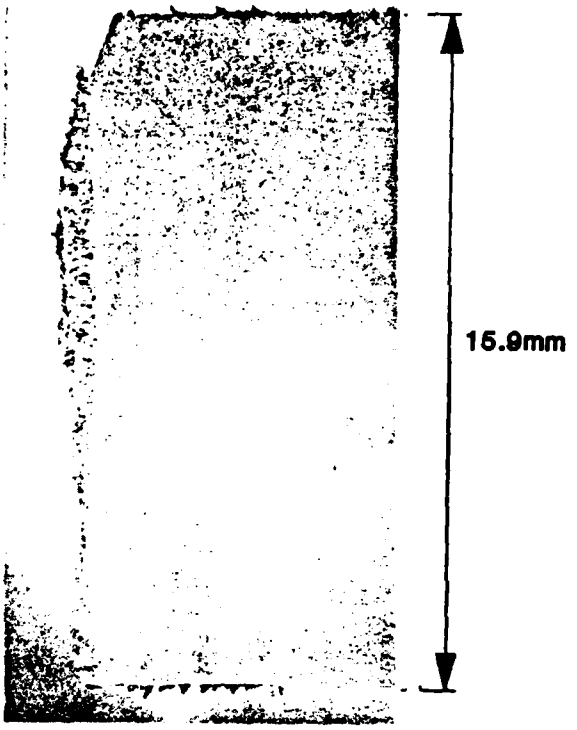

a) Macrograph showing cracking near edge of fusion zone

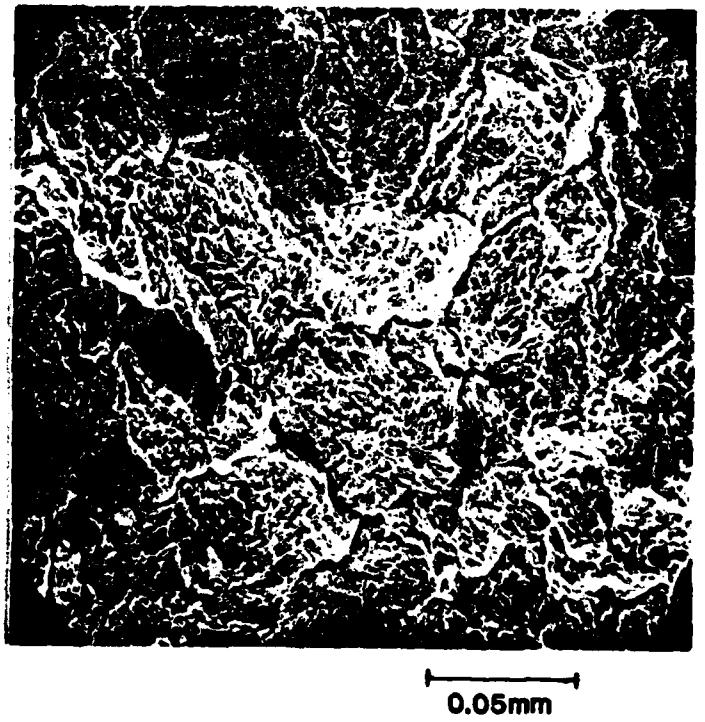

b) Scanning electron micrograph showing roughness of fracture surface and numerous branching microcracks

FIG 13. FUSION ZONE CRACK GROWTH AWAY FROM CENTRELINE IN LB WELD

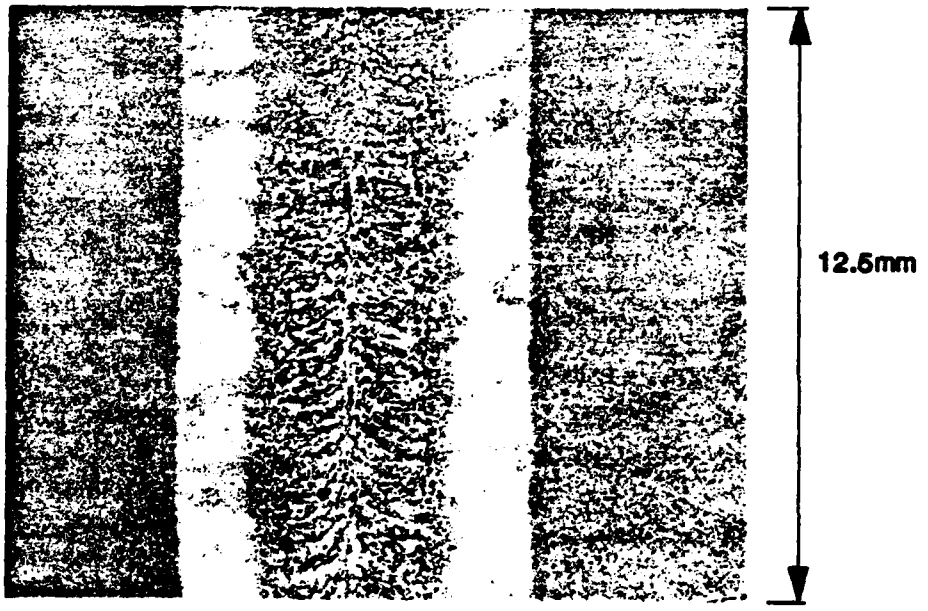

FIG 14. LONGITUDINAL MACROSECTION OF EB WELD

DISTRIBUTION

1. CS AMTE(HH)
2. D AMTE
3. Hd MC
4. Hds Divs Circulating Copy HH + Alverstoke + Vernon
5. Hd FDS
6. AMTE(S)
7-9. AMTE(S) (FAO Mr I Kilpatrick, Mr J Bird, Dr J Sumpter)
10. MC Registry
11. Mr D E McGeachie
12. Dr Culpan
13. RAL 6E
14. Package Coord 6E
15. DGS
16. Mat R Coord
17. DI53
18-19. Authors
20-30. AMTE Library
31. ASWE
32. AUWE
33. ERDE
34. MVEE Chertsey
35. MVEE Christchurch
36. RAE
37. The Welding Institute (FAO D Russell)
38. Vickers Shipbuilders and Engineers Ltd (FAO A Acheson)
39. Dr E Metzbower, NRL Washington, USA
40. Dr J Ritter MRL Melbourne, Australia
41-50. DRIC (1 copy for OS records)

END

FILMED

DTIC